A NUMERICAL EXPERIMENT OF THE PBL WITH GEOSTROPHIC MOMENTUM APPROXIMATION

Zhao Ming (赵 鸣)

Department of Atmospheric Sciences, Nanjing University, Nanjing

Received July 7, 1986

ABSTRACT

In this paper, a numerical experiment of the motion in the PBL (planetary boundary layer) is performed with geostrophic momentum approximation, in which a nonlinear eddy transfer coefficient is used. Some results are obtained for the boundary layer winds in cyclone-anticyclone and trough-ridge systems. This treatment improves W-B's work. The effects of geostrophic wind tendency and the advection of the geostrophic wind on the winds in the PBL are also discussed.

I. INTRODUCTION

The accurate simulation and forecasting of the winds in the PBL require a nonsteady three-dimensional numerical model, and their operation needs not only numerous calculations, but also needs three-dimensional initial and boundary conditions for which special observations have to be made. At present, this kind of work is performed only occasionally apart from some special experiments and research. In order to predict the wind field of the PBL on a large scale, diagnostic analysis was usually applied (Hadeen et al., 1972) ; i.e., by means of the geostrophic winds (or the winds at the top of the PBL) at grid points predicted by large or mesoscale models, the winds in the PBL were obtained from a steady and horizontally homogeneous PBL model. This procedure did not consider the advection and local variation in the PBL, so it was not rigorous. Wu and Blumen (1982) investigated the winds in the PBL by utilizing the geostrophic momentum approximation; the primary nonlinear nonsteady motion equations of the PBL were linearized, and the three-dimensional equations became one dimensional. This treatment not only considers the local and advection variations, but also does not need to solve the complicated three-dimensional equations, and the winds in the PBL can be calculated so long as the geostrophic wind, its spatial distribution and temporal tendency are known. The latter two can be predicted from a large-scale model. Obviously, this treatment has improved the computation of the wind distribution in the PBL. Furthermore, Wu (1985) investigated the effects of orography on the winds in the PBL by means of the geostrophic momentum approximation. In order to find the analytic solution, the constant K of classical Ekman theory was used in this work, hence the intrinsic defects of the Ekman model were also introduced in the results; i.e., the model results of the wind speeds in the lower PBL were too low to coincide with observations. This can be seen as follows: in the surface layer, the turbulent shear stress $\tau = K\frac{dV}{dz}$ should be constant according to micrometeorological concept, K is

proportional to the height in this layer, and consequently, $\frac{dV}{dz}$ must be large enough near the surface because K is small there. If $K=$constant is taken, then its value should be an appropriate medium magnitude in order that it can stand for the K in all the PBL; therefore, $\frac{dV}{dz}$ becomes small near the surface and the wind speed there will be too low. Furthermore, if $K=$ constant is taken, then $\frac{dV}{dz}$ will be equal to a constant in the surface layer. This results in wind speed being a linear function of height, which contradicts the logarithmic distribution of wind speed as is known. For example, we use Wu and Blumen's Eq. (57) to calculate the wind speed in the PBL at $r=1000$ km in the cyclone represented by their Eq. (56) (Wu and Blumen, 1982). There the geostrophic wind speed is 20.44 m/s, if $K=10$ m^2/s is taken, and as a result, a speed of 0.34 m/s is obtained at 6 m height and 0.65 m/s at 16 m in the cyclone. Obviously, these results do not coincide with observations (in reality the wind speed at 10 m is usually about half of the speed at the top of the PBL). From the viewpoint of application, Wu and Blumen's work could be improved.

In this paper, we use the geostrophic momentum approximation to treat the winds in the PBL, but the K expression from turbulent mixing length theory is used to calculate the friction terms in the PBL equations. This treatment retains the advantages of the geostrophic momentum approximation, but the more realistic transfer coefficient, compared with W-B's model, results in more realistic wind speed values. The eddy friction force is nonlinear because of the K, so that only numerical solutions can be obtained. However, the procedure for solving the equations is not complicated using our method.

II. GOVERNING EQUATIONS AND THEIR NUMERICAL INTEGRATION

According to the theory of geostrophic momentum approximation (Hoskins, 1975), the wind vector V_g in the individual variation term in the motion equation can be substituted by the geostrophic wind vector V_g when the inertia term is much smaller than the Coriolis terms in the motion equation (usually the large scale motion in medium and high latitudes is satisfied). When the friction force is neglected (at the top of the PBL), we have:

$$\frac{du_g}{dt}=fv-fv_a \tag{1}$$

$$\frac{dv_g}{dt}=fu_a-fu, \tag{2}$$

where u, v are the components of the wind vector and u_g, v_g, the geostrophic wind components, either f is the Coriolis parameter, or

$$u=-\frac{1}{f}\frac{dv_g}{dt}+u_a \tag{3}$$

$$v=\frac{1}{f}\frac{du_g}{dt}+v_g, \tag{4}$$

where

$$\frac{d}{dt}=\frac{\partial}{\partial t}-u\frac{\partial}{\partial x}+v\frac{\partial}{\partial y}. \tag{5}$$

Here we have neglected the small vertical advection terms. In Eqs. (3) and (4), the advected winds are substituted by the geostrophic winds and the advecting winds are still the original ones, i.e., the sum of the geostrophic winds and geostrophic departures. The winds in local variation terms are also substituted by the geostrophic winds. Equations (3) and (4) can be written as:

$$u=-\frac{1}{f}\left(\frac{\partial v_g}{\partial t}+u\frac{\partial v_g}{\partial x}+v\frac{\partial v_g}{\partial y}\right)+u_g \tag{6}$$

$$v=\frac{1}{f}\left(\frac{\partial u_g}{\partial t}+u\frac{\partial u_g}{\partial x}+v\frac{\partial u_g}{\partial y}\right)+v_g \tag{7}$$

u and v can be solved from Eqs. (6) and (7), and they are taken as the upper boundary condition u_T and v_T at the top of the PBL:

$$u_T=\frac{\left(u_g-\frac{1}{f}\frac{\partial v_g}{\partial t}\right)\left(1-\frac{1}{f}\frac{\partial u_g}{\partial y}\right)-\left(v_g+\frac{1}{f}\frac{\partial u_g}{\partial t}\right)\frac{1}{f}\frac{\partial v_g}{\partial y}}{1+\frac{1}{f}\left(\frac{\partial v_g}{\partial x}-\frac{\partial u_g}{\partial y}\right)+\frac{1}{f^2}\left(\frac{\partial u_g}{\partial x}\frac{\partial v_g}{\partial y}-\frac{\partial v_g}{\partial x}\frac{\partial u_g}{\partial y}\right)} \tag{8}$$

$$v_T=\frac{\left(v_g+\frac{1}{f}\frac{\partial u_g}{\partial t}\right)\left(1-\frac{1}{f}\frac{\partial v_g}{\partial x}\right)+\left(u_g-\frac{1}{f}\frac{\partial v_g}{\partial t}\right)\frac{1}{f}\frac{\partial u_g}{\partial x}}{1+\frac{1}{f}\left(\frac{\partial v_g}{\partial x}-\frac{\partial u_g}{\partial y}\right)+\frac{1}{f^2}\left(\frac{\partial u_g}{\partial x}\frac{\partial v_g}{\partial y}-\frac{\partial v_g}{\partial x}\frac{\partial u_g}{\partial y}\right)}. \tag{9}$$

Wu and Blumen (1982) applied the geostrophic momentum approximation to the PBL. In this case, obviously, only the large-scale features of the boundary layer are discussed; the boundary layer flow caused by local, small-scale inhomogeneous conditions (for example, the region near the interface between water and land) is not included, as it requires three-dimensional models. We use the same treatment as in W-B's work, but change their K expression. The motion equations of the PBL are:

$$\frac{\partial u_g}{\partial t}-u\frac{\partial u_g}{\partial x}-v\frac{\partial u_g}{\partial y}=f(v-v_g)-\frac{\partial}{\partial z}K\frac{\partial u}{\partial z} \tag{10}$$

$$\frac{\partial v_g}{\partial t}+u\frac{\partial v_g}{\partial x}+v\frac{\partial v_g}{\partial y}=-f(u-u_g)+\frac{\partial}{\partial z}K\frac{\partial v}{\partial z}. \tag{11}$$

Applying the generally used K expression in neutral conditions from mixing length theory (Blackadar, 1979), we have:

$$K=l^2\left[\left(\frac{\partial u}{\partial z}\right)^2+\left(\frac{\partial v}{\partial z}\right)^2\right]^{\frac{1}{2}} \tag{12}$$

$$l=\frac{0.4(z+z_0)}{1+\frac{0.4(z+z_0)}{\lambda}} \tag{13}$$

$$\lambda=0.0063\frac{u_*}{f} \tag{14}$$

$$u_*=\left(K\frac{dV}{dz}\right)^{\frac{1}{2}}_{z=z_1}, \tag{15}$$

where l is the mixing length, u_* is friction velocity, z_s is a height near the surface, and z_0 the roughness length (here 1 cm is taken, representing smooth surface). Of course, other z_0 may also be taken to determine the effects of the roughness. In practice, different z_0 can be taken at different horizontal coordinates. The neutral condition may represent the general condition of the boundary layer atmosphere. Equations (10)–(15) form a closed set of equations. Because of the geostrophic momentum approximation, the advection terms in Eqs. (10) and (11) have been linearized. On account of the nonlinear K in Eq. (12), the motion equations must be solved numerically, but this is not difficult.

The lower boundary condition is:

$$u = v = 0 \qquad \text{where} \qquad z = 0 \tag{16}$$

The upper boundary condition should be the wind at the top of the PBL determined from Eqs. (8) and (9):

$$u = u_T, \quad v = v_T \qquad \text{where} \qquad z = h, \tag{17}$$

h is the upper boundary of the PBL; here 1000 km is chosen. This upper boundary condition differs from those modern boundary layer models in which the wind at the upper boundary is taken to be geostrophic wind. Eq. (17) is more reasonable because the individual variation of the geostrophic wind is not zero in a nonsteady and horizontally inhomogeneous model.

Now we solve Eqs. (10)–(15) under conditions (16) and (17). $\frac{\partial u_g}{\partial t}$, $\frac{\partial v_g}{\partial t}$ and the horizontal gradients of the geostrophic wind components are considered to be known from large scale variation of pressure field. The equation system is similar to the one-dimensional one, but the effects of nonsteady and horizontal inhomogeneity have been included through the geostrophic momentum approximation.

The vertical grid point coordinates are listed in Table 1.

Table 1. The Vertical Grid Point Coordinates

No.	1	2	3	4	5	6	7	8	9	10	11	12	13	14	15	16
z(m)	0	0.25	0.5	1	2	6	16	32	64	100	200	300	400	600	800	1000

where u and v are defined at these grid points and K at the midways between the grid points. It is not difficult to transform Eqs. (10) and (11) into difference equations and solve them by means of the method used in steady and horizontally homogeneous problems (Zhao, 1983). The successive approximation method has been used; i.e., we choose K = constant, for example, 10 m^2/s at first, and solve Eqs. (10) and (11). After the first approximations $u^{(1)}$, $v^{(1)}$ are obtained, we substitute them into Eqs. (12)–(15) to calculate $u_*^{(1)}$, $\lambda^{(1)}$, $l^{(1)}$, $K^{(1)}$, then solve Eqs. (10), (11) again to obtain $u^{(2)}$, $v^{(2)}$, then $K^{(2)}$,... The method of Zhao (1983) can make the iterative process converge quickly. Usually, 20 iterations can give a relative error of 10^{-3}, 10 iterations can give an error of 1%, and, at the same time, K, u_* and other boundary parameters are solved.

III. COMPUTATIONAL EXAMPLE: CYCLONE AND ANTICYCLONE

As an example, we solve the wind distribution of the PBL in the following circularly symmetrical cyclone and anticyclone as assumed by Wu and Blumen (1982):

$$\phi = \pm\left(1 - \frac{a}{2}r^2\right)e^{-\frac{a}{2}r^2}, \tag{18}$$

where "−" represents cyclone and "+", anticyclone, $\alpha=0.5$, r the nondimensional radius, and ϕ the nondimensional geopotential deviation. Assuming the Rossby number $Ro=0.3$, horizontal length scale $L=10^3$ km, $f=10^{-4}s^{-1}$, and horizontal velocity scale $U=30$ m/s. With $K=10$ m^2/s, [as in Wu and Blumen (1982)], we calculate the wind speeds u, v at $x=10^6$ m and $y=0$ (here the origin is located at the center of the cyclone or anticyclone, x axis points forward to east, y axis to north) which are represented by the symbol "△" and a dashed line in Figures (1) and (2). The numbers beside these symbols represent their heights (m) beginning from 16 m. The numbers beside other symbols represent the heights of all other different symbols

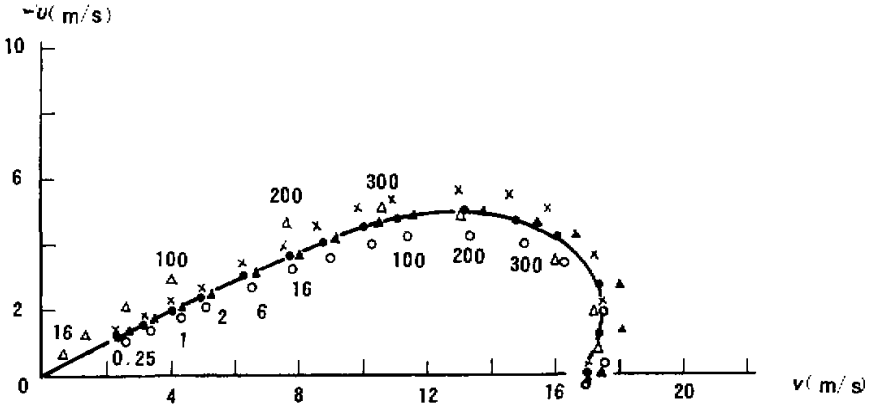

Fig. 1. The distribution of PBL wind in cyclone.
△ W-B's solution
▲ 3D model solution
× $\frac{\partial v_g}{\partial t}>0$, ○ $\frac{\partial v_g}{\partial t}<0$,
• $\frac{\partial v_g}{\partial t}=0$

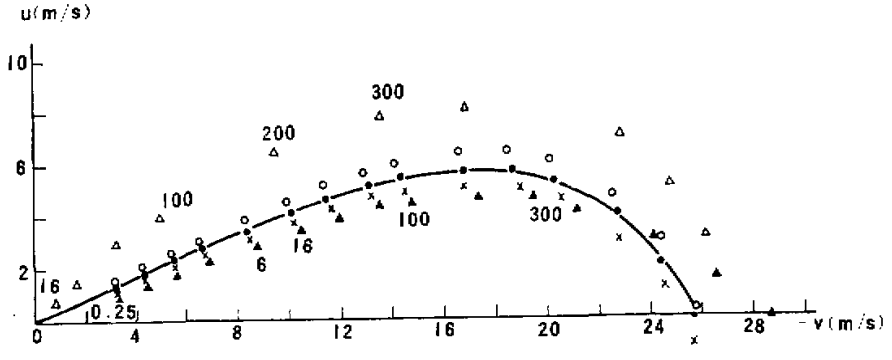

Fig. 2. The distribution of PBL wind in anticyclone; the legend is identical to that of Fig. 1.

beginning from 0.25 m; i.e., they represent the solution when K is taken as Eq. (12).

Our solutions in the steady case $\left[\frac{\partial u_g}{\partial t}=\frac{\partial v_g}{\partial t}=0 \text{ in Eqs. (10) and (11)}\right]$ are represented by the solid line and dots in these figures. From Figs. 1 and 2, it is seen that W-B's solution gives much smaller values of wind speed at lower heights than ours. Our angles between the wind vectors near the surface and isobars are smaller than 45°, giving more realistic results. For example, in our results, the wind speed at 10 m is about 8 m/s in cyclone, 11 m/s in anticyclone (corresponding geostrophic wind is 17 m/s in cyclone and 28.6 m/s in anticyclone). Zhao (1983) had obtained the numerical solutions of three-dimensional boundary layer equations in a circular vortex with the same K as in this paper, but the gradient winds at the upper boundary were assumed not to change with radius. It is not difficult to extend those solutions to the case where the gradient winds at the upper boundary are a function of the radius, (i.e., the gradient wind is an arbitrary function of radius). We can obtain this numerical solution of the three-dimensional boundary layer model when the gradient winds at the upper boundary are derived from Eq. (18) without using the geostrophic momentum approximation. Compared with the geostrophic momentum approximation, these solutions represented by symbols "▲" in Figs. (1) and (2) may be considered to be rigorous and accurate because all the nonlinear advection terms are computed.

It can be seen that the similarity between the solutions in this paper and the three-dimensional solutions is stronger than that between W-B's solutions and the latter. It is concluded that our results not only are accurate, but also save computation time, and thus are an improvement on W-B 's work.

We may discuss the effects of the geostrophic wind tendency on the solutions of Eqs. (10) and (11) if we take $\frac{\partial u_g}{\partial t}$ and $\frac{\partial v_g}{\partial t}$ into account. In Figs. 1 and 2, the results taking $\frac{\partial v_g}{\partial t}=\pm 8$ ms^{-1}/24 h at the same location are shown. It is found that in cyclone, $|u|$ for the case of $\frac{\partial v_g}{\partial t}>0$ is larger than that for $\frac{\partial v_g}{\partial t}=0$; i.e., the value of u is smaller, and vice versa for the case of $\frac{\partial v_g}{\partial t}<0$. This can be explained as follows: when $\frac{\partial v_g}{\partial t}>0$ in Eq.(11), it is equivalent to putting $\frac{\partial v_g}{\partial t}=0$ in Eq. (11) and at the same time make the value of fu_g on the r.h.s. decrease by $\frac{\partial v_g}{\partial t}$, the decrease of u_g(or the increase of the absolute value of u_g) causes the wind component in x direction to decrease (or the absolute value of u to increase). The result for the case of $\frac{\partial v_g}{\partial t}<0$ can also be explained as above. In the anticyclone, all the results turn out contrary to the case of the cyclone, and may also be explained in the same way ($u>0$ in anticyclone).

Therefore, from the solution obtained by the method of geostrophic momentum approximation, we may indirectly infer the characteristics of PBL wind distribution from the steady PBL wind distributions when the geostrophic wind tendencies are not zero.

IV. COMPUTATIONAL EXAMPLE: TROUGH-RIDGE SYSTEM

Now we consider the solutions in trough-ridge systems. We solve the wind distribution problems in the east of a trough and a ridge. For simplicity, we assume that the geostrophic wind corresponding to the trough-ridge system at a certain time is a simple sinusoidal wave:

$$u_g = \text{const}, \qquad v_g = \text{const} \sin \frac{2\pi}{L} x \tag{19}$$

where L is the wave length, x axis points forward to the east and y axis to the north, the east of the trough corresponds to $0<x<\frac{L}{2}$ and the east of the ridge to $\frac{L}{2}<x<L$, and:

$$\frac{\partial v_g}{\partial x}>0 \qquad \text{where} \quad 0<x<\frac{L}{4}$$

$$\frac{\partial v_g}{\partial x}<0 \qquad \text{where} \quad \frac{L}{4}<x<\frac{L}{2}$$

$$\frac{\partial v_g}{\partial x}<0 \qquad \text{where} \quad \frac{L}{2}<x<\frac{3L}{4}$$

$$\frac{\partial v_g}{\partial x}>0 \qquad \text{where} \quad \frac{3L}{4}<x<L.$$

As an individual example, some regions located in the east of the trough and bounded by $\frac{L}{4}<x<\frac{L}{2}$ are considered. The PBL wind distribution in the case where $u_g=15$ m/s, $v_g=5$ m/s, and $\frac{\partial v_g}{\partial x}=-5$ ms^{-1}/1000 km is shown by the solid line in Fig.3, where the dashed line depicts the wind distribution in a steady horizontally homogeneous PBL without using the geostrophic momentum approximation and its upper boundary wind components are u_g and v_g. It is shown from Fig. 3 that the u solution using the geostrophic momentum approximation with horizontal inhomogeneity is larger than that horizontally homogeneous solution, especially in the upper part of the PBL. Because the value of $\frac{\partial v_g}{\partial x}$ is not large enough in the above example, this difference is not yet significant. This phenomenon can be explained as follows: from Eq.(11), $u\frac{\partial v_g}{\partial x}<0$ because $\frac{\partial v_g}{\partial x}<0$; this is equivalent to putting $u\frac{\partial v_g}{\partial x}=0$ in Eq. (11) and at the same time making fu_g on the r.h.s. increase, i.e. making u_g increase causes the wind component in x direction to increase also. This is similar to the examples for cyclone and anticyclone in the last section. Hence, wind distribution in the PBL may be inferred indirectly from the wind in the steady and horizontally homogeneous PBL and the latter has been investigated sufficiently so far. Again, we discuss the effects of the geostrophic wind tendency. Assuming $\frac{\partial u_g}{\partial t}=\pm 5$ ms^{-1}/24 h and $\frac{\partial v_g}{\partial t}=0$, as shown in

Fig. 3, we find that v increases as $\frac{\partial u_g}{\partial t}>0$ and decreases as $\frac{\partial u_g}{\partial t}<0$. These characteristics can be explained from Eq. (10). $\frac{\partial u_g}{\partial t}>0$ is equivalent to putting $\frac{\partial u_g}{\partial t}=0$ in Eq. (10) and at the same time making $-fv_g$ on the r.h.s. decrease; i.e., making v_g increase results in increasing v. The results of $\frac{\partial u_g}{\partial t}<0$ can be explained analogously. If we put $\frac{\partial u_g}{\partial t}=0$ and $\frac{\partial v_g}{\partial t}=\pm 2$ ms^{-1}/24 h, as shown in Fig. 3, u decreases as $\frac{\partial v_g}{\partial t}>0$ and increases as $\frac{\partial v_g}{\partial t}<0$; the reason for this can be found from Eq. (11).

In the east of the trough bounded by $0<x<\frac{L}{4}$ where $\frac{\partial v_g}{\partial x}>0$, the difference of the wind in this region from the steady and homogeneous PBL wind is quite the reverse of the case where $\frac{\partial v_g}{\partial x}<0$, but the effects of $\frac{\partial u_g}{\partial t}$ and $\frac{\partial v_g}{\partial t}$ are the same. We shall not discuss this in

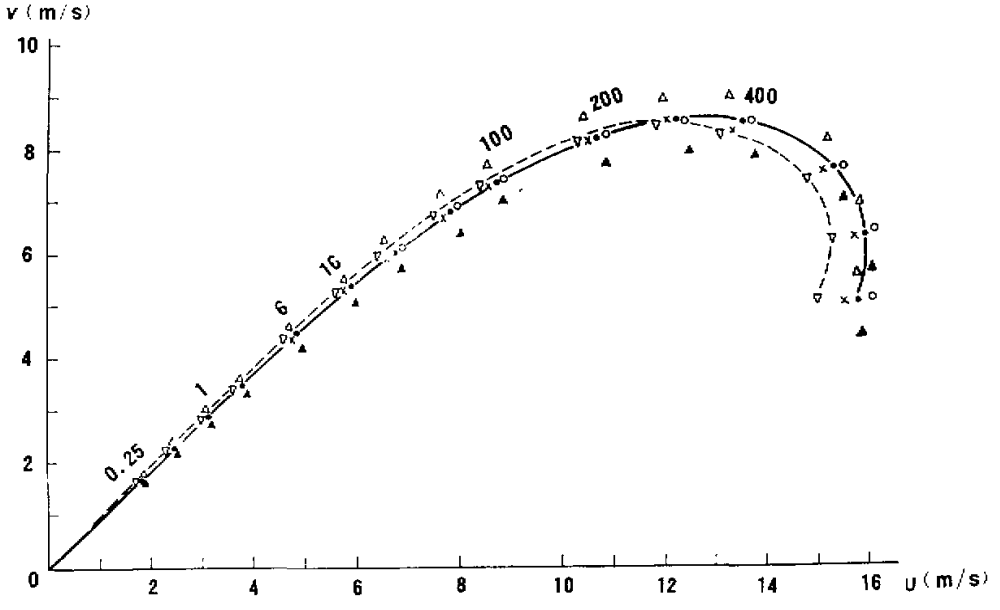

Fig. 3. The boundary layer wind in the east of trough and $\frac{\partial v_g}{\partial x}<0$,
▽———the steady and homogeneous solution.
·—— $\frac{\partial}{\partial t}=0$, × $\frac{\partial v_g}{\partial t}>0$, ○ $\frac{\partial v_g}{\partial t}<0$,
△ $\frac{\partial u_g}{\partial t}>0$, ▲ $\frac{\partial u_g}{\partial t}<0$.

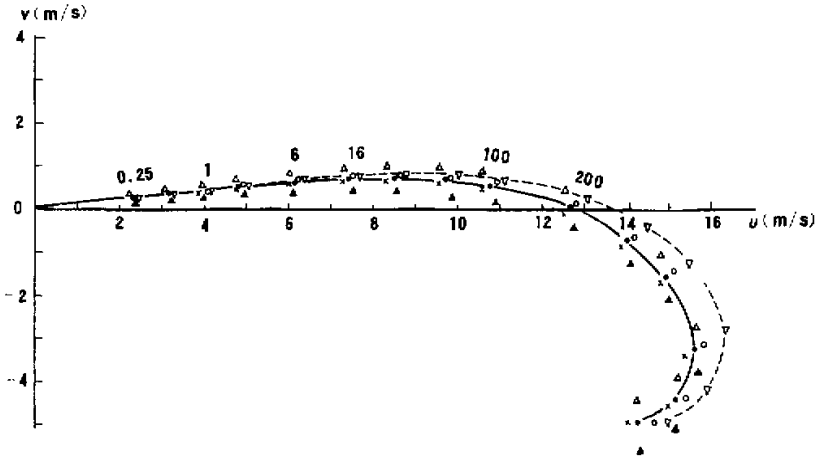

Fig. 4. The boundary layer wind in the east of ridge and $\frac{\partial v_g}{\partial x}>0$, the legend is identical to that of Fig. 3.

detail here.

Figure 4 gives the results for the locations in the east of the ridge bounded by $\frac{3L}{4}<x<L$ where $\frac{\partial v_g}{\partial x}>0$, assuming $u_g=15$ m/s, $v_g=5$ m/s and $\frac{\partial v_g}{\partial x}=5$ ms^{-1}/1000 km. Comparing with the steady and horizontally homogeneous solution, u is found to be smaller. From Eq. (11), $u\frac{\partial v_g}{\partial x}>0$. This is equivalent to making u_g decrease in the steady and homogeneous solution, and results in decreasing u; it is opposite to the case in the region in the east of the trough. Again, if we put $\frac{\partial u_g}{\partial t}=\pm 5$ ms^{-1}/24 h and $\frac{\partial v_g}{\partial t}=\pm 2$ ms^{-1}/24 h, we can obtain the same conclusion as in the trough case. If the region is bounded by $\frac{L}{2}<x<\frac{3L}{4}$, then $\frac{\partial v_g}{\partial x}<0$. The results may be easily deduced analogously.

V. SUMMARY

In this paper, assuming that the spatial distribution and temporal tendency of the geostrophic wind are known and using the K expression in the friction terms from the mixing length theory, we have treated the motion equations of the PBL with geostrophic momentum approximation, simplified the three-dimensional primary equations into one-dimensional equations, and the wind distribution in the PBL is thus obtained. This treatment retains the advantage of the method of Wu and Blumen (1982) and at the same time gives more precise results. The geostrophic wind tendency and spatial distribution of the geostrophic wind may be found

from large scale models. We have computed several examples such as cyclone-anticyclone, and trough-ridge systems, and obtained the differences between PBL winds in these pressure systems and those in horizontally homogeneous conditions (i.e., the isobars are parallel straight lines). These differences may be explained completely by the motion equations. The wind distributions in the steady and horizontally homogeneous conditions have been investigated sufficiently, so that the PBL wind distribution in different systems can be inferred from the steady and homogeneous PBL wind by use of the geostrophic wind tendency and the spatial distribution of the geostrophic wind.

The treatment in this paper is not suited to small-scale boundary layer problems and only the wind distribution in neutral and barotropic conditions is discussed here. In principle, the treatment here can also be applied to non-neutral and baroclinic conditions if the non-neutral K expression is used and the effects of the baroclinity to the pressure gradient force in the motion equations are introduced. Therefore, the numerical experiment method discussed here is a general one.

REFERENCES

Blackadar, A.K. (1979), High resolution models of the PBL, in J.R. Pfaff'lin and E.N. Ziegler (eds), Advances in Environmental Science and Engineering, 1, Gorden and Breach, 50—85.

Hadeen, K.D. and Friend, A. (1972), The air force global weather central operational boundary layer model. *Boundary Layer Meteorol.*, **2**:98—112.

Hoskins, B.J. (1975), The geostrophic momentum approximation and the semi-geostrophic equations. *J. Atmos. Sci.*, **32**:233—242.

Wu, R. (1985), The influences of orography upon the flow within Ekman boundary layer under the approximation of geostrophic momentum. *Adv. Atmos. Sci.*, **2**:1—7.

Wu,R and Blumen, W. (1982), An analysis of Ekman boundary layer dynamics incorporating the geostrophic momentum approximation. *J. Atmos. Sci.*, **39**:1174—1182.

Zhao, M. (1983), The theoretical distribution of wind in the PBL with circular isobars. *Boundary Layer Meteorol.*, **26**:209—226.